Journal of Cerebral Blood Flow & Metabolism (2014) 34, 1907–1913

www.jcbfm.com

ORIGINAL ARTICLE

In vivo imaging of reactive oxygen species in mouse brain by using [^{3}H]Hydromethidine as a potential radical trapping radiotracer

Kohji Abe[1], Nozomi Takai[1], Kazumi Fukumoto[2], Natsumi Imamoto[1], Misato Tonomura[1], Miwa Ito[1], Naoki Kanegawa[1], Katsunori Sakai[2], Kenji Morimoto[2], Kenichiro Todoroki[3] and Osamu Inoue[4]

To assess reactive oxygen species (ROS) production by detecting the fluorescent oxidation product, hydroethidine has been used extensively. The present study was undertaken to evaluate the potential of the hydroethidine derivative as a radiotracer to measure *in vivo* brain ROS production. [^{3}H]-labeled *N*-methyl-2,3-diamino-6-phenyl-dihydrophenanthridine ([^{3}H]Hydromethidine) was synthesized, and evaluated using *in vitro* radical-induced oxidization and *in vivo* brain ROS production model. *In vitro* studies have indicated that [^{3}H]Hydromethidine is converted to oxidized products by a superoxide radical ($O_2^{\bullet}-$) and a hydroxyl radical ($OH^{\bullet}-$) but not hydrogen peroxide (H_2O_2). *In vivo* whole-body distribution study showed that [^{3}H]Hydromethidine rapidly penetrated the brain and then was washed out in normal mice. Microinjection of sodium nitroprusside (SNP) into the brain was performed to produce ROS such as $OH^{\bullet}-$ via Fenton reaction. A significant accumulation of radioactivity immediately after [^{3}H]Hydromethidine injection was seen in the side of the brain treated with SNP (5 and 20 nmol) compared with that in the contralateral side. These results indicated that [^{3}H]Hydromethidine freely penetrated into the brain where it was rapidly converted to oxidized forms, which were trapped there in response to the production of ROS. Thus, [^{3}H]Hydromethidine should be useful as a radical trapping radiotracer in the brain.

Journal of Cerebral Blood Flow & Metabolism (2014) **34,** 1907–1913; doi:10.1038/jcbfm.2014.160; published online 17 September 2014

Keywords: *in vivo* molecular imaging; radical trapping radiotracer; reactive oxygen species

INTRODUCTION

Reactive oxygen species (ROS) have a pivotal role as regulatory mediators in signal processes at moderate concentrations.[1] An excessive amount of ROS causes the imbalance of redox state and damages cell function in living tissue and organs. A sustained increase in ROS production has been implicated in a wide variety of disease state such as inflammation, cancer, ischemia/reperfusion injury, neurodegenerative disorders, and oxidative stress.[2–5] The superoxide radical ($O_2^{\bullet}-$) is usually the primary ROS produced and is subsequently converted into hydrogen peroxide (H_2O_2) through spontaneous or superoxide dismutase (SOD)-catalyzed dismutation. Reaction of $O_2^{\bullet}-$ and nitric oxide (NO) generates peroxynitrite ($ONOO^{\bullet}-$). Reaction of H_2O_2 and $ONOO^{\bullet}-$ can generate the highly reactive hydroxyl radical ($OH^{\bullet}-$).[6,7] $O_2^{\bullet}-$ is subsequently converted into $OH^{\bullet}-$ and H_2O_2.[8] To clarify the roles of different ROS in disease pathogenesis, highly sensitive and specific optical probes (fluorescent, luminescent, or chemiluminescent probes) for detecting ROS are being developed.[9–12]

Hydroethidine, a fluorescent ROS probe, is extensively used in tissue experiments (*in vitro* and *ex vivo*) to detect $O_2^{\bullet}-$ production. The reaction between hydroethidine and $O_2^{\bullet}-$ is considered to generate an oxidative product with red fluorescence.[13–15] Hydroethidine, an uncharged lipophilic compound is easily transported to a tissue or a cell, where it is converted to positively charged products (membrane-impermeable products), which become trapped there. Murakami *et al.*[16] have reported that hydroethidine can detect the $O_2^{\bullet}-$ produced by occlusion of the middle cerebral artery using mutant mice with a heterozygous knock-out gene encoding mitochondrial manganese SOD. It has also been reported to detect $O_2^{\bullet}-$ production in the hippocampus of lithium-pilocarpine epilepsy rats,[17] beta cells of type II diabetes mellitus rats,[18] or the brain of multiple sclerosis mice.[19]

Recently, Hall *et al.*[20] have reported the detection of $O_2^{\bullet}-$ production in real time in aging or ketamine-pretreated brain using an optical imaging technique with hydroethidine and fluorescence lifetime contrast-based unmixing. This optical imaging is useful as a relatively simple method to detect the production of $O_2^{\bullet}-$ but quantitative measurement is difficult with respect to tissue absorption of the optical signal. Generally, a radiolabeled probe such as ^{3}H or ^{14}C is used to acquire quantitative autoradiogram with high sensitivity. Probe-labeled positron emitters such as ^{11}C or ^{18}F enable noninvasive measurement of the whole body. Radiotracer of hydroethidine-related compounds is considered to be trapped in tissue based on the hypothesis of metabolic trapping as reaction between hydroethidine and ROS results in the generation of a cation-charged product, the oxidized form of hydroethidine.

In the present study, we synthesized ^{3}H-labeled hydromethidine and evaluated its ability to detect ROS *in vitro* and *in vivo*.

[1]Research Laboratory for Development, Department of Drug Metabolism and Pharmacokinetics, Shionogi & Co., Ltd, Osaka, Japan; [2]Research Laboratory for Development, Department of Applied Chemistry and Analysis, Shionogi & Co., Ltd, Osaka, Japan; [3]Department of Analytical and Bio-Analytical Chemistry, School of Pharmaceutical Sciences, University of Shizuoka, Shizuoka, Japan and [4]School of Allied Health Sciences, Faculty of Medicine, Osaka University, Osaka, Japan. Correspondence: Dr K Abe, Research Laboratory for Development, Department of Drug Metabolism and Pharmacokinetics, Shionogi & Co., Ltd, 3-1-1 Futaba, Toyonaka, Osaka 561-0825, Japan.
E-mail: kohji.abe@shionogi.co.jp
Received 29 July 2014; revised 25 August 2014; accepted 26 August 2014; published online 17 September 2014

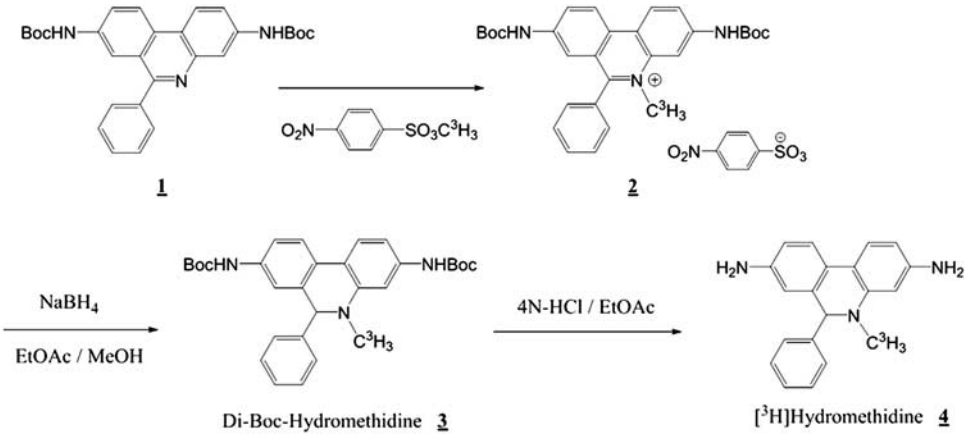

Figure 1. Labeling scheme for [^{3}H]Hydromethidine.

Hydromethidine was selected as a prototype of radiotracer since it is possible to synthesize ^{3}H and ^{11}C-labeled compounds by *N*-methylation. *In vivo* brain ROS generation was performed by striatal microinjection of sodium nitroprusside (SNP) generating ROS including $OH^{\bullet}-$ by Fenton reaction.[21] The $OH^{\bullet}-$ is one of the most reactive ROS in neuronal tissue damage.

MATERIALS AND METHODS

Animals

All animal experiments in the present study were reviewed and approved by the Institutional Animal Care and Use Committee of Shionogi Research Laboratories (Osaka, Japan) and were consistent with the internal guidelines for animal experiments and in adherence to the ethics policy of Shionogi & Co., Ltd (Osaka, Japan). Male C57BL/6 J mice were purchased from CLEA Japan, Inc. (Tokyo, Japan) and were 8 weeks old at the time of experiments. They were allowed free access to chow and tap water and housed in a temperature-controlled room maintained on a 12-hour light/dark cycle with lights on at 0800 h.

Chemicals and Reagents

$NaBH_4$, 3,8-diamino-6-phenanthridine, hypoxanthine, xanthine oxidase, and SOD were obtained from Sigma-Aldrich (St Louis, MO, USA). [methyl-^{3}H] Methyl nosylate was obtained from Perkin-Elmer, Inc. (Waltham, MA, USA). Ethyl acetate (EtOAc), n-hexane, CH_3COONH_4, and dimethyl sulfoxide (DMSO) were obtained from Nacalai Tesque (Kyoto, Japan), and 4N-HCl/EtOAc from Watanabe Chemical Industries Ltd. (Hiroshima, Japan). PIC B8 low UV was obtained from Waters Corp. (Milford, MA, USA). Acetonitrile, $NaHCO_3$, and $FeSO_4{\cdot}7H_2O$ were obtained from Kanto Chemical Co. Inc. (Tokyo, Japan). Di-*tert*-butyl dicarbonate ($(Boc)_2O$), H_2O_2, and sodium pentacyanonitrosylferrate (III) dihydrate (SNP) were obtained from Wako Pure Chemical Industries Ltd. (Osaka, Japan). Isoflurane was from Abbott Japan Co., Ltd. (Tokyo, Japan), and NOC-18 from Dojindo Laboratories (Kumamoto, Japan).

Synthesis of [^{3}H]Hydromethidine

The radiochemical reaction was monitored by high performance liquid chromatography (HPLC) system (LC-20A; Shimadzu, Kyoto, Japan) with a flow scintillation analyzer (Radiomatic 625TR; Perkin-Elmer, Inc.).

Labeling scheme for [^{3}H]Hydromethidine is shown in Figure 1. Starting material (**1**) was prepared by treating 3,8-diamino-6-phenanthridine with $(Boc)_2O$. [methyl-^{3}H]Methyl nosylate (total activity: 370 MBq, specific activity: 740 GBq/mmol) and starting material (**1**) were dissolved in acetonitrile and stirred at 80°C for 5 hours. The reaction mixture was purified by preparative thin-layer chromatography (SiO_2 60 F_{254}; Merck, Darmstadt, Germany) using EtOAc as a developing solvent, and extracted with EtOAc/methanol (2:1) to give di-Boc-methidium 4-nitrobenzene-sulfonate (**2**). Di-Boc methidium 4-nitirobenzenesulfonate was reduced by $NaBH_4$ to give di-Boc-Hydromethidine (**3**), and deprotected with 4N HCl/EtOAc solution. The reaction mixture was concentrated, mixed with $NaHCO_3$ aq. to adjust the pH to about 8, and extracted with EtOAc. The extract was purified by preparative thin-layer chromatography (Chromatorex DNH, Fuji Silysia Chemical Ltd., Aichi, Japan) using n-hexane/EtOAc (1:2) as developing solvents to give a solution of [^{3}H]Hydromethidine (**4**). Specific activity was measured by liquid chromatography/mass spectrometry system (Quattro micro ESCi with Alliance 2690 and 2487 Dual Absorbance Detector; Waters Corp.). Radiochemical purity was measured by a radio-HPLC system using a Cadenza CD-C18 column (40°C, 3 μm, 3.0 × 75 mm; Imtakt Corp., Kyoto, Japan) eluted at 0.4 mL/min with a gradient of A (CH_3COONH_4 buffer containing 5 mmol/L PIC B8 low UV, pH 4.5) and B (acetonitrile), with B being increased linearly from 30% to 90% (v/v) over 15 minutes. Specific activity and radiochemical purity were 74 GBq/mmol and 98.8%, respectively. For the following experiments, [^{3}H] Hydromethidine was diluted with distilled water containing 5% DMSO (v/v), giving 95.7% of radiochemical purity.

In vitro Reaction Between [^{3}H]Hydromethidine and Reactive Oxygen Species

The hypoxanthine/xanthine oxidase system was used to generate $O_2^{\bullet}-$. Hypoxanthine (0.42 mmol/L) containing [^{3}H]Hydromethidine was incubated with xanthine oxidase (8.3 mU/mL) in phosphate-buffered saline (2.7 mmol/L KCl, 137 mmol/L NaCl, 10 mmol/L phosphate, pH 7.4) at 37°C for 20 minutes. Superoxide dismutase (250 U/mL) was used to scavenge the generated $O_2^{\bullet}-$.

The Fenton reaction was used to generate $OH^{\bullet}-$. Fe^{2+} (1.7 mmol/L) containing [^{3}H]Hydromethidine was incubated with H_2O_2 (74 mmol/L) in distilled water at room temperature for 20 minutes.

The radioactivity of an aliquot of each mixture after the incubation was measured with a liquid scintillation analyzer (Perkin-Elmer, Inc.). Another aliquot of the mixture was mixed with an equal volume of EtOAc before centrifugation (11 000 *g*, 4°C, 3 minutes), and the radioactivity of the organic layer was measured. The values are expressed as % remaining of [^{3}H]Hydromethidine calculated by dividing the weight-corrected radioactivity of the organic layer by that of the incubated mixture.

Whole-Body Distribution in Mice

An aqueous solution (5% DMSO, v/v) of [^{3}H]Hydromethidine (74 kBq) was injected intravenously into the tail vein of mice. The mice were killed by decaptation at postinjection time points of 1, 5, 10, 30, and 60 minutes under deep anesthesia with isoflurane, and the organs of interest were removed. The tissue weights were determined, and the radioactivity in the tissue was measured with a liquid scintillation analyzer (Perkin-Elmer, Inc.). The percentage of unmetabolized [^{3}H]Hydromethidine in the radioactivity of blood was determined as follows. The radioactivity of an aliquot of blood samples was measured with a liquid scintillation analyzer. Another aliquot of blood samples was mixed with 2 mL of EtOAc, and the radioactivity of the organic layer was measured. The values are calculated by dividing the weight-corrected radioactivity of the organic layer by that of the blood sample. Remaining blood samples were centrifuged at 11 000 *g* for 3 minutes at 4°C to obtain plasma.

Intrastriatal Injection of Sodium Nitroprusside and NOC-18

Injection of SNP or NOC-18 into the striatum of mice was performed using a stereotactic apparatus under isoflurane anesthesia. Sodium nitroprusside (5 or 20 nmol/μL; dissolved in saline) or NOC-18 (20 nmol/μL; dissolved in phosphate-buffered saline) was injected into the right striatum using a 25-μL syringe with a 33-gauge needle controlled by an automated syringe pump at a rate of 0.25 μL/min for 4 minutes. The coordinates for the stereotactic injection were 0.74 mm anterior, 1.6 mm lateral, and 3.5 mm ventral from the bregma, according to the atlas of Paxinos and Franklin.[22] After the injection, the needle was kept in the same position for an additional 3 minutes to allow diffusion of drugs and then retrieved slowly from the brain. At the same time, 1 μL of saline for SNP or phosphate-buffered saline for NOC-18 was injected into the left striatum by the same method.

Autoradiography

At 60 and 30 minutes after the intrastriatal injection of SNP and NOC-18, respectively, an aqueous solution (5% DMSO, v/v) of [^{3}H]Hydromethidine (740 kBq) was injected intravenously into the tail vein of mice. The mice were killed by decapitation at postinjection time points of 1, 5, 20, or 60 minutes under deep anesthesia with isoflurane. The brains were rapidly removed and frozen, and sections (2 μm thick) were prepared using a cryostat. The sections were exposed to an imaging plate (BAS-TR; Fujifilm Corp., Tokyo, Japan) for 14 days. After exposure, the plates were read with a FLA-3000 (Fujifilm Corp.). Regions of interest were drawn on the images, and the photo-stimulated luminescence value for each region of interest (PSL/mm^2) was determined using Multi Gauge version 2.3 (Fujifilm Corp.).

RESULTS

In Vitro Oxidation Characteristic of [^{3}H]Hydromethidine

[^{3}H]Hydromethidine was oxidized by $O_2^{\bullet}-$ produced with hypoxanthine and xanthine oxidase. Superoxide dismutase, which rapidly removes $O_2^{\bullet}-$, inhibited the oxidation of [^{3}H]Hydromethidine (Figure 2A). [^{3}H]Hydromethidine showed oxidation in the presence of $OH^{\bullet}-$ as shown in Figure 2B. However, its oxidation was not observed in the presence of H_2O_2.

Whole-Body Distribution in Mice Intravenously Injected with [^{3}H] Hydromethidine

We examined the tissue distribution after intravenous injection of [^{3}H]Hydromethidine into normal mice as shown in Figure 3. [^{3}H] Hydromethidine rapidly penetrated the cell membranes including the blood–brain barrier, with high uptake by the brain, lungs, and heart immediately after the injection of the [^{3}H]Hydromethidine. In the brain, almost homogeneous distribution as well as rapid clearance of radioactivity was observed in all regions. The radioactivity in the lungs, heart, and muscles also disappeared, while relatively high levels of radioactivity remained in the liver during

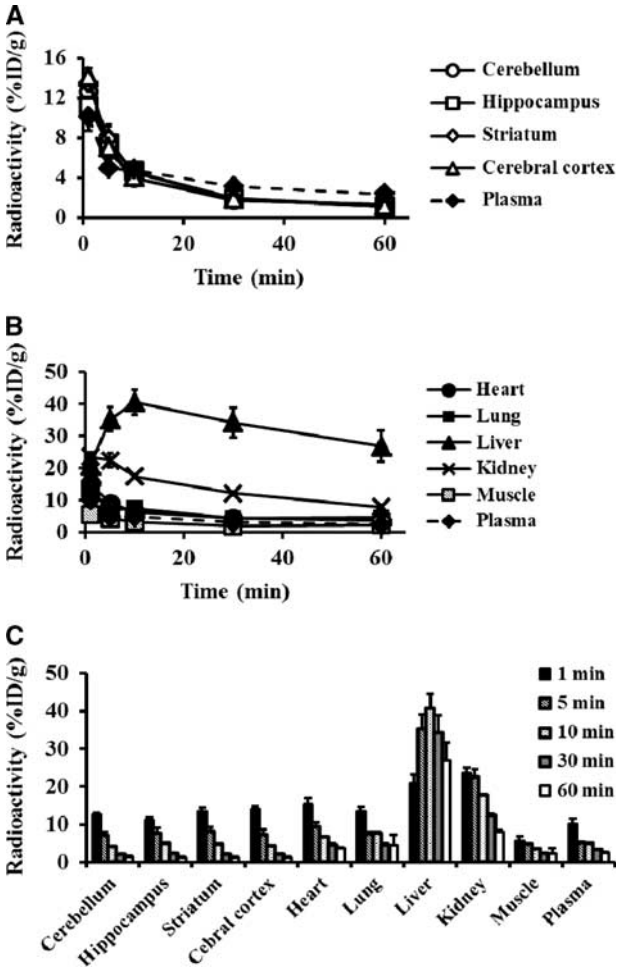

Figure 3. Distribution profiles of radioactivity in the brain (**A**) and other tissues (**B** and **C**) after intravenous injection of [^{3}H] Hydromethidine to mice. Data are expressed as %ID/g (mean ± s.d., $n = 3$).

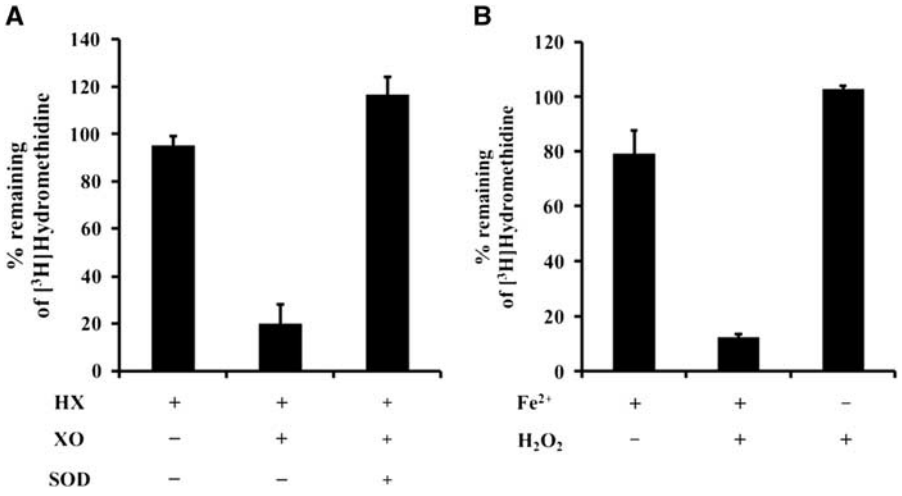

Figure 2. *In vitro* reactivity of [^{3}H]Hydromethidine with reactive oxygen species (ROS) produced by hypoxanthine (HX)/xanthine oxidase (XO) system (**A**) or Fenton reaction (**B**). Data are expressed as % remaining of [^{3}H]Hydromethidine after incubation (mean ± s.d., $n = 3$). Superoxide dismutase (SOD) was used to remove $O_2^{\bullet}-$.

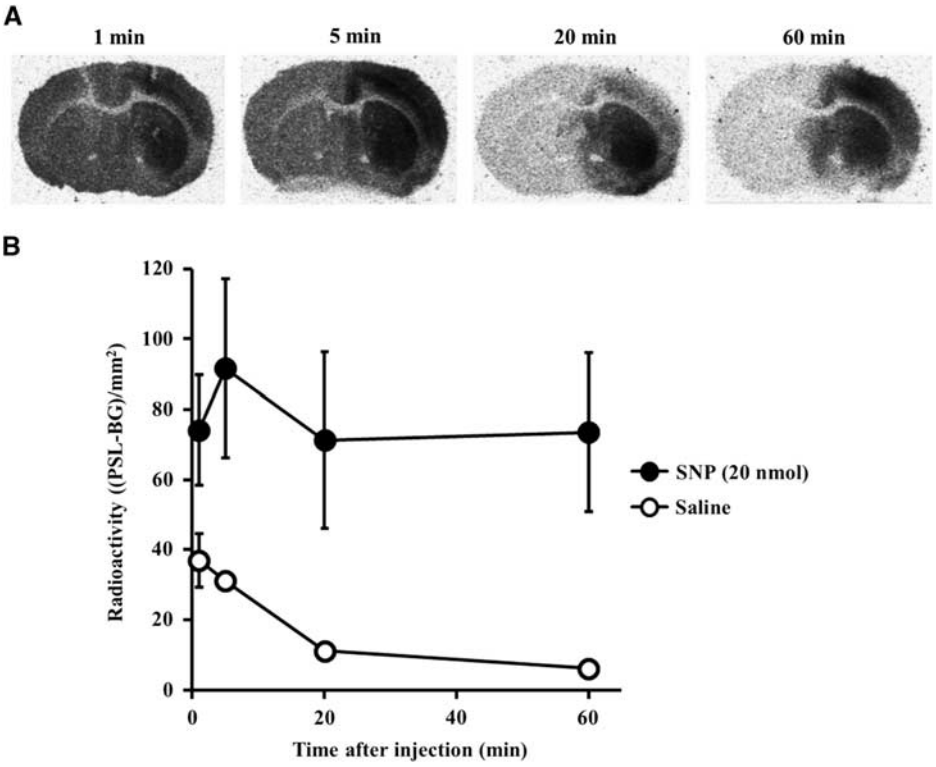

Figure 4. Accumulation of radioactivity in the brain after intravenous injection of [3H]Hydromethidine to mice treated with sodium nitroprusside (SNP) (20 nmol). SNP was microinjected to the right striatum. (**A**) Typical autoradiograms in brain obtained at 1, 5, 20, and 60 minutes after [3H]Hydromethidine injection. (**B**) Radioactivity profiles in the SNP-injected striatum (●) and saline-injected striatum (○), calculated from the autoradiograms. Data are expressed as (PSL-BG)/mm^2 (mean ± s.d., $n = 4$).

the 60-minute observation period. The percentage of unmetabolized [3H]Hydromethidine in the radioactivity of blood was 95.1 ± 27.7%, 73.1 ± 13.4%, 59.9 ± 6.8%, 55.8 ± 4.6%, and 56.7 ± 9.9% at 1, 5, 10, 30, and 60 minutes, respectively, postinjection of [3H] Hydromethidine.

Brain Distribution after Intravenous Injection of [3H] Hydromethidine in Mice Given Intrastriatal Microinjection of Sodium Nitroprusside

Typical autoradiograms obtained 1, 5, 20, and 60 minutes after [3H]Hydromethidine injection to mice treated with SNP (20 nmol) are shown in Figure 4. In the SNP-treated hemisphere, high accumulation of radioactivity was sustained during 60 minutes of period. In contrast, rapid decline in radioactivity accumulation in the contralateral hemisphere was observed. In the striatum, the ratios of radioactivity concentrations of the SNP-injected side to the contralateral side were 2.0 at 1 minute, 6.6 at 20 minutes, and 12.2 at 60 minutes after [3H]Hydromethidine injection.

The degree of radioactivity accumulation at 60 minutes after injection of [3H]Hydromethidine was much dependent on the dose (5 or 20 nmol) of SNP. No significant difference of radioactivity concentrations was observed between the right and left hemispheres of mouse brain injected with NOC-18 (Figure 5).

Figure 6 shows the brain distribution in SNP-microinjected mice when the oxidized product of [3H]Hydromethidine was intravenously injected. The oxidized product of [3H]Hydromethidine was acquired by generated $O_2^{\bullet}-$ using hypoxanthine/xanthine oxidase system *in vitro* and analyzed by radio-HPLC according to the method reported previously[11] with slight modifications. The oxidized product of [3H]Hydromethidine was estimated to consist mainly of methidium cation in comparison with the retention of

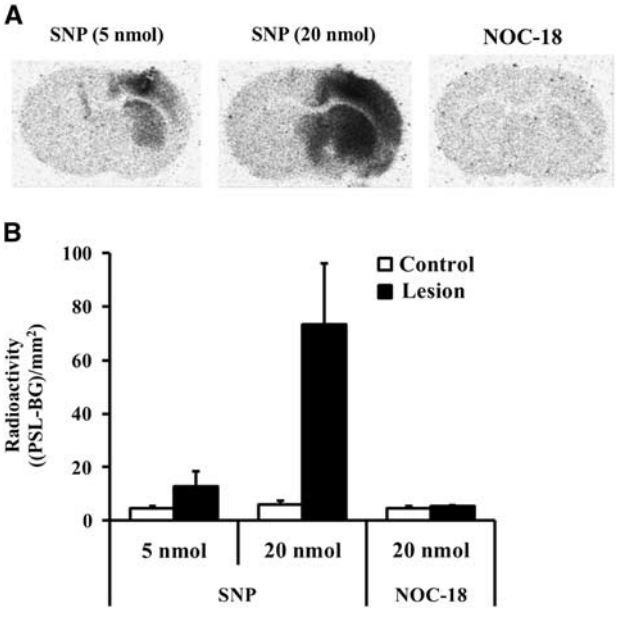

Figure 5. Accumulation of radioactivity in brain after intravenous injection of [3H]Hydromethidine to mice treated with sodium nitroprusside (SNP) (5 or 20 nmol) or NOC-18 (20 nmol). SNP or NOC-18 was microinjected to the right striatum. (**A**) Typical autoradiograms in brain obtained at 60 minutes after [3H]Hydromethidine injection. (**B**) Results of quantitative analysis of the autoradiograms. Radioactivity in the SNP or NOC-18-injected striatum (■) and control striatum (□) was calculated and expressed as (PSL-BG)/mm^2 (mean ± s.d., $n = 4$).

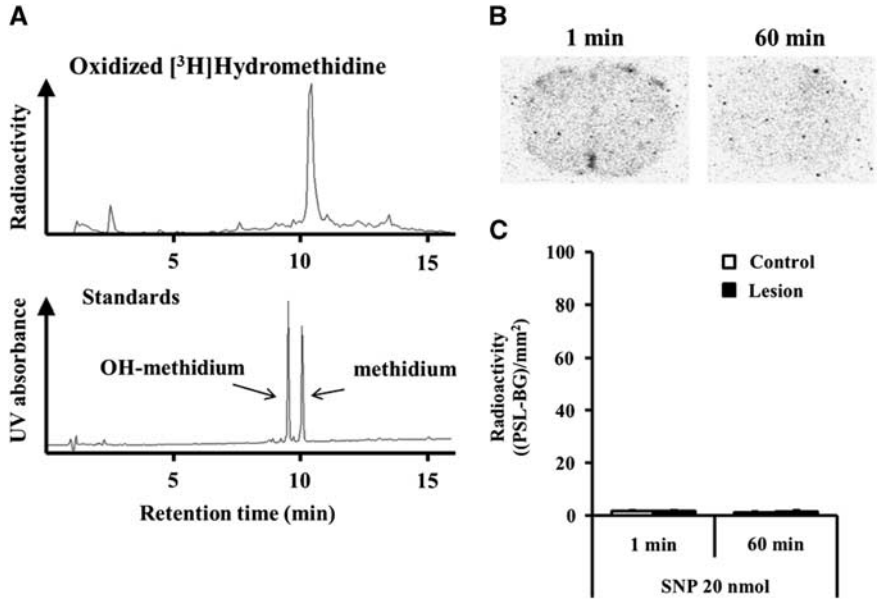

Figure 6. Accumulation of radioactivity in brain after intravenous injection of oxidized product of [3H]Hydromethidine to mice treated with sodium nitroprusside (SNP) (20 nmol). SNP was microinjected to the right striatum. (**A**) Radio-HPLC analysis of oxidized [3H]Hydromethidine solution for administration. Oxidized Hydromethidine standards were also analyzed by HPLC-UV. (**B**) Typical autoradiograms in brain obtained at 1 and 60 minutes after oxidized product of [3H]Hydromethidine injection. (**C**) Results of quantitative analysis of the autoradiograms. Radioactivity in the SNP-injected striatum (■) and control striatum (□) was calculated and expressed as (PSL-BG)/mm^2 (mean ± s.d., $n = 3$). HPLC, high performance liquid chromatography.

synthesized methidium cation or hydroxymethidium cation detected by UV.

When the oxidized product was intravenously injected into mice, no significant uptake of radioactivity was observed in the brain, which indicates that the oxidation metabolite of [3H] Hydromethidine did not penetrate the blood–brain barrier due to its cationic charge.

DISCUSSION

We found that [3H]Hydromethidine had the desired characteristic of a radical trapping probe based on the results of whole body kinetics as well as autoradiography of brain injected with SNP after injection of [3H]Hydromethidine tracer. [3H]Hydromethidine was rapidly distributed to organs such as brain, heart, and lung after tracer injection. This was followed by its rapid clearance from the organs for normal mouse tissue. In the brain, a significantly high accumulation of radioactivity in the SNP-injected side (striatum and cerebral cortex) was seen even at 1 minute after injection of the tracer and the radioactivity concentrations were kept almost the same level during 60 minutes of period. In contrast, the radioactivity in the contralateral normal side (saline-injected side) of the brain was rapidly disappeared. In addition, the extent of radioactivity accumulation in the SNP-injected side was much dependent on the injected dose of SNP. It has been reported that SNP caused cell death dose-dependently when microinjected into the striatum.[23] In addition, cell death induced by intrastriatal microinjection of SNP was caused by iron-related ROS such as $OH^{\bullet}-$ via the Fenton reaction but not by NO or CN. Rauhala *et al.*[21] also showed that SNP generated $OH^{\bullet}-$ by the Fenton reaction *in vitro* in the presence of ascorbate. We have also reported that intrastriatal microinjection of SNP (50 nmol) caused neuronal cell death; however, neither NOC-18 (50 nmol), another type of NO donor, nor sodium cyanide (50 nmol) caused cell death.[24] The accumulation of radioactivity observed in the SNP-injected side suggests that [3H]Hydromethidine was oxidized by ROS such as $OH^{\bullet}-$ and then the oxidized form was trapped in the tissue. It is possible that [3H]Hydromethidine was also oxidized by other ROS since SNP generates not only $OH^{\bullet}-$ but also $O_2^{\bullet}-$, NO, or $ONOO^{\bullet}-$.[25] In addition, lipid peroxidation of cell membrane induced by ROS is considered to oxidize [3H]Hydromethidine in intact tissues. As for the involvement of NO radical, we found that no accumulation of radioactivity was seen in the NOC-18-injected side. In this experiment, 20 nmol of SNP is considered to release 20 nmol of NO under the optimum conditions, whereas 40 nmol of NO might be released by 20 nmol of NOC-18. The NO-generating ability of NOC-18 has been reported to be greater than that of SNP.[26] However, NOC-18 is a relatively slow NO donor that has a prolonged half-life of 20 hours. Therefore, the optimal dose and time for the treatment of NO donor is important for controlling NO level under the *in vivo* conditions. Further studies on the reactivity of [3H]Hydromethidine with reactive nitrogen species such as NO and $ONOO^{\bullet}-$ both *in vitro* and *in vivo* will be needed. This result of NOC-18 suggests that oxidation of [3H]Hydromethidine may not be mediated by NO under at least the present experimental conditions. Thus, the accumulation of radioactivity induced by SNP is considered to be mainly due to oxidative conversion of [3H] Hydromethidine by ROS such as $OH^{\bullet}-$.

We also investigated whether the oxidative products of [3H] Hydromethidine, which had been oxidized in the presence of xanthine oxidase and hypoxanthine, were able to penetrate into the brain. We found that the oxidative product produced by generation of $O_2^{\bullet}-$ was mostly the [3H]Hydromethidium cation. The *in vitro* ROS reactivity study suggests that the reaction between [3H]Hydromethidine and $OH^{\bullet}-$ or $O_2^{\bullet}-$ produces its oxidative forms. The results with SNP-treated mice clearly showed that [3H]Hydromethidine was easily transported to a tissue or a cell and converted to a membrane-impermeable oxidization product, which became trapped there. A significant accumulation of radioactivity in the SNP-injected brain strongly suggests that the oxidized form of [3H]Hydromethidine produced by $OH^{\bullet}-$ or $O_2^{\bullet}-$ was trapped in the brain. Hydroethidine has been reported

to be rapidly distributed into the tissues including the brain[16,27] and the oxidation products are retained in cells in the brain. These findings suggest that hydroethidine-related compounds can serve as radical trapping radiotracer. In addition, the autoradiography study indicated that entered [^{3}H]Hydromethidine in the brain was rapidly oxidized to cationic form and trapped in the brain. As the input function (unoxidized [^{3}H]Hydromethidine in the brain) rapidly declined with time, the conversion of [^{3}H]Hydromethidine in the brain seemed to be almost completed within few minutes after the bolus injection. The amount of trapped oxidized form was mainly dependent on three factors, the delivery process from plasma (regional blood flow), the oxidation rate in the brain, and the washout rate of unoxidized [^{3}H]Hydromethidine from the brain. As previously reported that no significant effects on cerebral blood flow were observed in rat brain injected with SNP (50 nmol/μL),[28] the delivery process from the plasma seemed to be unaffected by SNP injection. The washout rate of unoxidized [^{3}H]Hydromethidine from the brain was rapid. Therefore, the amount of trapped oxidized form in the brain seemed to be dependent on the oxidation rate in the brain.

Brain ROS have been implicated in a variety of pathophysiologic conditions such as Alzheimer's disease, Parkinsonism, multiple sclerosis, ischemia-reperfusion injury, and brain trauma.[29,30] As mentioned above, [^{3}H]Hydromethidine is considered to be a useful probe for assessing the role of ROS in the pathologic brain state. We have been able to confirm the accumulation of [^{3}H] Hydromethidine suggesting production of ROS in the rodent ischemia-reperfusion model (in preparation). Although we focused on the brain ROS in this study, the use of [^{3}H]Hydromethidine is not restricted to the central nervous system. The rapid clearance of [^{3}H]Hydromethidine in several tissues of control mice suggests that it might be possible to detect the ROS in peripheral tissues such as the lungs, heart, and kidney. Further studies will be needed to detect ROS in peripheral tissues considering the relatively high distribution in the liver. A high level of ROS production has also been reported in cancer tissue. Jung *et al.*[31] have reported a positive relationship between the uptake of ^{18}F-FDG and the level of ROS in tumor cells. In tumor cells, upregulated anaerobic metabolism, known as the Warburg effect,[32] was observed. There may be a close relation between this change in metabolism and ROS production. These reports suggest the usefulness of [^{3}H]Hydromethidine for assessing the role of ROS in tumor tissues and cells. [^{3}H]Hydromethidine was also thought to be useful for assessing ROS in tumor animal models because of its low uptake by mouse skeletal muscle.

Superoxide radical ($O_2^{\bullet}-$), primary ROS species, is subsequently converted into H_2O_2 through spontaneous or SOD-catalyzed dismutation. The reaction of $O_2^{\bullet}-$ and NO generates the powerful oxidant $ONOO^{\bullet}-$. Reaction of H_2O_2 and $ONOO^{\bullet}-$ can give rise to highly reactive $OH^{\bullet}-$.[6,7] Therefore, it is also important to know the selectivity and intensity of the radical trapping probe for the type of ROS. We found that [^{3}H]Hydromethidine reacted with $O_2^{\bullet}-$ and $OH^{\bullet}-$ but not with H_2O_2 from the results of *in vitro* study. Hydroethidine is widely used as an ROS probe specifically for $O_2^{\bullet}-$. As described above, dynamic optical imaging showed that brain $O_2^{\bullet}-$ was increased in SOD-deficient mice or ketamine-treated mice. In addition, the product of hydroethidine oxidation produced by $O_2^{\bullet}-$ *in vivo* was ethidium, not 2-hydroxyethidium from analysis of the fluorescence life time when hydroethidine was intravenously injected into mice at a dose of 50 mg/kg. Recent *in vitro* studies have suggested that the specific oxidation product of hydroethidine by $O_2^{\bullet}-$ is not ethidium, but 2-OH ethidium.[11] In the present study, the oxidative product of [^{3}H]Hydromethidine in the presence of hypoxanthine and xanthine oxidase was found to be mostly the [^{3}H]Hydromethidium cation. Several ROS such as $OH^{\bullet}-$ or $O_2^{\bullet}-$ might be produced by SNP treatment because of complex conditions of *in vivo* systems. The sensitivity of [^{3}H] Hydromethidine also seemed to be high since the injected dose was 0.15 mg/kg if calculated based on the specific activity. Further studies will be needed on the effects of the differences of the specific activity for detecting ROS.

Generally, radiolabeled probes are highly sensitive and quantitative. A metabolic trapping tracer using oxidative conversion would allow the amount of ROS produced in a given tissue or cell to be quantified by measurement of the oxidized products produced over a defined period. As shown in Figure 3, the radioactivity level at 60 minutes after tracer injection is considered to be an indicator of ROS level since unmetabolite of [^{3}H]Hydromethidine was mostly eliminated from the brain. In addition, Patlak plot analysis of the brain radioactivity concentrations enables calculation of the relative ROS amount when the kinetics of the unmetabolite of [^{3}H]Hydromethidine in plasma is used as the input function.

Noninvasive measurement using [^{3}H]-labeled compounds is not possible because of the low energy of beta rays. Time-dependent change in ROS could be detected in the same animals using positron-labeled hydroethidine-related compounds because Hydromethidine can be labeled using [^{11}C]methylation instead of [^{3}H] labeling. Therefore, small animal positron emission tomography (PET) studies using [^{11}C]Hydromethidine should be very useful for studying the pathophysiologic roles of ROS in diseases.

The present study showed that radiolabeled hydromethidine could enable assessment of ROS levels for treatments of inflammation and ischemia in animals. To the best of our knowledge, this is the first report showing the usefulness of radical trapping radiotracers for detecting brain ROS *in vivo*.

DISCLOSURE/CONFLICT OF INTEREST

The authors declare no conflict of interest.

REFERENCES

1 Droge W. Free radicals in the physiological control of cell function. *Physiol Rev* 2002; **82**: 47–95.
2 Hensley K, Robinson KA, Gabbita SP, Salsman S, Floyd RA. Reactive oxygen species, cell signaling, and cell injury. *Free Radic Biol Med* 2000; **28**: 1456–1462.
3 Hall ED, Andrus PK, Althaus JS, Vonvoigtlander PF. Hydroxyl radical production and lipid peroxidation parallels selective post-ischemic vulnerability in gerbil brain. *J Neurosci Res* 1993; **34**: 107–112.
4 Sayre LM, Smith MA, Perry G. Chemistry and biochemistry of oxidative stress in neurodegenerative disease. *Curr Med Chem* 2001; **8**: 721–738.
5 Valko M, Leibfritz D, Moncol J, Cronin MTD, Mzur M, Telser J. Free radicals and antioxidants in normal physiological functions and human disease. *Int J Biochem Cell Biol* 2007; **39**: 44–84.
6 Cadenas E. Biochemistry of oxygen toxicity. *Annu Rev Biochem* 1989; **58**: 79–110.
7 Hogg N, Darley-Usmar M, Wilson MT, Moncada S. Production of hydroxyl radicals from the simultaneous generation of superoxide and nitric oxide. *Biochem J* 1992; **281**: 419–424.
8 Ide T, Tsutsui H, Kinugawa S, Suematsu N, Hayashidani S, Ichikawa K *et al.* Mitochondrial oxidative stress in heart failure. *Circ Res* 2000; **86**: 152–157.
9 Asano M, Doi M, Baba K, Taniguchi M, Shibano M, Tanaka S *et al.* Bio-imaging of hydroxyl radicals in plant cells using the fluorescent molecular probe rohdamine B hydrazide, without any pretreatment. *J Biosci Bioeng* 2014; **118**: 98–100.
10 Michalski R, Zielonka J, Hardy M, Joseph J, Kalyanaraman B. Hydropropidine: A novel, cell-impermeant fluorogenic probe for detecting extracellular superoxide. *Free Radic Biol Med* 2013; **54**: 135–147.
11 Michalski R, Michalowski B, Sikora A, Zielonka J, Kalyanaraman B. On the use of fluorescence lifetime imaging and dihydroethidium to detect superoxide in intact animals and ex vivo tissues: a reassessment. *Free Radic Biol Med* 2014; **67**: 278–284.
12 Zhao H, Kalivendi S, Zhang H, Joseph J, Nithipatikom K, Vasquez-Vivar J *et al.* Superoxide reacts with hydroethidine but forms a fluorescent product that is distinctly different from ethidium: potential implications in intracellular fluorescence detection of superoxide. *Free Radic Biol Med* 2003; **34**: 1359–1368.
13 Barbacanne MA, Souchard JP, Darblade B, Iliou JP, Nepveu F, Pipy B *et al.* Detection of superoxide anion released extracellularly by endothelial cells using cytochrome c reduction, ESR, fluorescence and lucigenin-enhanced chemiluminescence techniques. *Free Radic Biol Med* 2000; **29**: 388–396.

14 Fernandes DC, Wosniak J, Jr, Pescatore LA, Bertoline MA, Liberman M, Laurindo FR *et al*. Analysis of DHE-derived oxidation products by HPLC in the assessment of superoxide production and NADPH oxidase activity in vascular systems. *Am J Physiol Cell Physiol* 2007; **292**: C413–C422.
15 Fink B, Laude K, McCann L, Doughan A, Harrison DG, Dikalov S. Detection of intracellular superoxide formation in endothelial cells and intact tissues using dihydroethidium and an HPLC-based assay. *Am J Physiol Cell Physiol* 2004; **287**: C895–C902.
16 Murakami K, Kondo T, Kawase M, Li Y, Sato S, Chen SF *et al*. Mitochondrial susceptibility to oxidative stress exacerbates cerebral infarction that follows permanent focal cerebral ischemia in mutant mice with manganeses superoxide dismutase deficiency. *J Neurosci* 1998; **18**: 205–213.
17 Pestana RRF, Kijo ER, Hernandes MS. Britto LRG. Reactive oxygen species generated by NADPH oxidase are involved in neurodegeneration in the pilocarpine model of the temporal lobe epilepsy. *Neurosci Lett* 2010; **484**: 187–191.
18 Bindokas VP, Kuznetsov A, Sreenan S, Polonsky KS, Roe MW, Philipson LH. Visualizing superoxide production in normal and diabetic rat islets of Langerhans. *J Biol Chem* 2003; **278**: 9796–9801.
19 Kim DY, Hao J, Liu R, Turner G, Shi FD, Rho JM. Inflammation-mediated memory dysfunction and effects of ketogenic diet in murine model of multiple sclerosis. *PLoS ONE* 2012; **7**: e35476.
20 Hall DJ, Han SH, Chepetan A, Inui EG, Rogers M, Dugan LL. Dynamic optical imaging of metabolic and NADPH oxidase-derived superoxide in live mouse brain using fluorescence lifetime unmixing. *J Cereb Blood Flow Metab* 2012; **32**: 23–32.
21 Rauhala P, Khaldi A, Mohanakumar KP, Chiueh CC. Apparent role of hydroxyl radicals in oxidative brain injury induced by sodium nitroprusside. *Free Radic Biol Med* 1998; **24**: 1065–1073.
22 Paxinos G, Franklin KBJ. *The mouse brain in stereotaxic coordinates*; 2nd edn. Academic Press: San Diego
23 Nazari OA, Mizumo K, Kume T, Takada-Takatori Y, Izumi Y, Akaike Y. In vivo brain oxidative stress model induced by microinjection of sodium nitroprusside in mice. *J Pharmacol Sci* 2012; **120**: 105–111.
24 Yanamoto K, Hosoi R, Uesaka Y, Abe K, Tsukada H, Inoue O. Intrastriatal microinjection of sodium nitroprusside induces cell death and reduces binding of dopaminergic receptors. *Synapse* 2003; **50**: 137–143.
25 Aleryani S, Milo E, Kostka P. Formation of peroxynitrite during thiol-mediated reduction of sodium nitroprusside. *Biochim Biophys Acta* 1999; **1472**: 181–190.
26 Tanno M, Sueyoshi S, Miyata N, Nagkagawa S. Nitric oxide generation from aromatic N-nitrosoureas at ambient temperature. *Chem Pharm Bull* 1996; **44**: 1849–1852.
27 Quick KL, Dugan LL. Superoxide stress identifies neurons at-risk in a model of ataxia-telangiectasia. *Ann Neurol* 2001; **49**: 627–635.
28 Inoue O, Taguchi H, Watanabe T, Hosoi R, Kobayashi K, Nishimura T *et al*. Uncoupling of flow and metabolism induced by sodium nitroprusside in rat cerebral cortex. *Neuroreport* 2004; **15**: 141–145.
29 Choi BY, Jang BG, Kim JH, Lee BE, Sohn M, Song HK *et al*. Prevention of traumatic brain injury-induced neuronal death by inhibition of NADPH oxidase activation. *Brain Res* 2012; **1481**: 49–58.
30 Jenner P. Oxidative stress in Parkinson's disease. *Ann Neurol* 2003; **53**: S26–S36.
31 Jung KH, Lee JH, Quach CHT, Paik JY, Oh H, Park JW *et al*. Resveratrol suppresses cancer cell glucose uptake by targeting reactive oxygen species-mediated hypoxia-inducible factor-1α activation. *J Nucl Med* 2013; **54**: 2161–2167.
32 Warburg O. On respiratory impairment in cancer cells. *Science* 1956; **124**: 269–270.